Full Length Article

Study of the conversion of CH_4/H_2S mixtures at different pressures

J.M. Colom-Díaz, M. Leciñena, A. Peláez, M. Abián, Á. Millera, R. Bilbao, M.U. Alzueta *

Aragón Institute of Engineering Research (I3A), Department of Chemical and Environmental Engineering, University of Zaragoza, 50018 Zaragoza, Spain

ARTICLE INFO

ABSTRACT

Due to the different scenarios where sour gas is present, its composition can be different and, therefore, it can be exploited through different processes, being combustion one of them. In this context, this work deals with the oxidation of CH_4 and H_2S at different pressures and under a wide variety of conditions. The oxidation has been evaluated experimentally in two different flow reactor set-ups, one working at atmospheric pressure and another one operating from atmospheric to high pressures (40 bar). Different CH_4/H_2S mixtures have been tested, together with different oxygen concentrations and in the temperature range of 500–1400 K. The experimental results obtained show that the oxidation of the CH_4/H_2S mixtures is shifted to lower temperatures as pressure increases, obtaining the same trends at atmospheric pressure in both experimental set-ups. H_2S oxidation occurs prior to CH_4 oxidation at all conditions, providing radicals to the system that promote CH_4 oxidation to lower temperatures (compared to neat CH_4 oxidation). This effect is more relevant as pressure increases. H_2S oxidation is inhibited by CH_4 at atmospheric pressure, being more noticeable when the CH_4/H_2S ratio is higher. At higher pressures, the H_2S conversion occurs similarly in the absence or presence of CH_4. The experimental results have been modeled with an updated kinetic model from previous works from the literature, which, in general, matches well the experimental trends, while some discrepancies between experimental and modeling results at atmospheric pressure and 40 bar are found in the conversion of H_2S and CH_4.

1. Introduction

Recently, the International Energy Agency has paid special attention to natural gas, exploring how the rise of shale gas and natural gas reserves is changing the global gas market, as well as the opportunities and risks for gas use in the transition to cleaner energy systems [1]. The abundance of natural gas reserves can facilitate the transition from fossil derived to fully renewable fuels [2,3]. Unconventional sources, such as sour and shale gas (natural gas with significant amounts of H_2S and CO_2, up to 30% content in volume each [4]), are becoming more important and bring interest to the direct use of these fuels, with the consequent development of proper combustion processes and technologies for their utilization, including the necessity of an increase of the knowledge and understanding of their conversion under high pressure conditions [5].

The high CO_2 content, as well as the presence of hydrogen sulfide (H_2S), limit the economic and environmental viability of sour gas resources. So far, the main solution has relied upon the production of sulfur through sulfur recovery units (SRU) using acid gas, that includes both CO_2 and H_2S [6], based on the Claus process [7], performing thus a prior cost effective separation process from the fuel. In these units, the H_2S is partially oxidized, producing both SO_2 and S that further re-

act in the Claus reactor in the presence of a catalyst. CH_4 might be added to the process to increase furnace temperature and preventing flame extinction [8]. Improvements of the Claus process include: the use of oxygen enrichment, as it raises the flame temperature by eliminating the diluent effect of nitrogen in air [9], production of hydrogen or syngas together with sulfur in the Claus process [10,11], or sulfur production from SO_2 containing streams, by reaction of SO_2 with methane to produce CS_2 and H_2S, and later on sulfur [12].

Another possibility for natural gas utilization, particularly shale gas containing significant amounts of H_2S, is its direct combustion. Not many studies on that are available in the literature. Actually, to our knowledge, only oxy-combustion of sour gas has been addressed in the literature [13–15], including the development of this process at high pressures to increase efficiency in power plants [16,17]. The high-pressure conditions may allow the direct use of sour gas in a gas turbine process [13].

Apart from sour gas reserves, H_2S is also present together with CH_4 in biogas obtained from the anaerobic biochemical conversion of biomass, in a range of 100–10000 ppm [18]. As increasing the share of renewable energy is considered to be one of the main options to reduce greenhouse gas emissions, energy from biomass has the potential to provide power to the grid on demand, for example, using biogas combustion in gas turbines [19], which can tolerate a H_2S content up

to 10000 ppm [18]. However, this issue has not been deeply investigated yet [20].

It is clear that conversion of CH_4/H_2S mixtures under combustion conditions is an important research topic. In particular, studies carried out under high pressure conditions are necessary because of turbine combustion applications. In this context, both experimental studies and kinetic modeling development to describe the conversion of CH_4/H_2S mixtures can be of great interest and usefulness.

All in all, to go further into the knowledge of the combustion behavior of H_2S under different conditions, it exists a need for the development of comprehensive kinetic models that can capture the combustion chemistry of H_2S, as well as the co-oxidation of CH_4 and H_2S, which remain unknown in many aspects, while the available experimental data are limited. Previous studies of co-oxidation of CH_4/H_2S mixtures have considered mainly Claus process conditions (this is, 1–1.5 bar, 1075–1350 K) [21,22]. The only study at high pressures is the recent work from Gersen et al. [23], where they studied experimentally the autoignition and oxidation of CH_4/H_2S mixtures in a rapid compression machine (RCM) and a flow reactor. They showed prediction results with their model that agree well with the measured autoignition delay times. On the other hand, the authors indicated that the H_2S oxidation chemistry and the interaction of CH_4 and H_2S at high pressure are not well understood, emphasizing that more work is desirable on the reactions of H_2S and SH with peroxides (HO_2 and CH_3OO) and the formation and consumption of organosulfur compounds. The kinetic mechanism used in the work of Gersen et al. [23] is based on the works from Hashemi et al. [24] for CH_4 oxidation and Song et al. [25] about H_2S oxidation at high pressures.

While the conversion of methane is known with a certain confidence, more work is desirable regarding the H_2S oxidation. The current mechanisms used for H_2S oxidation [e.g. 13–15,26] are mainly based on the work from Zhou et al. [27], which has been used for describing H_2S oxidation in recent works, addressing ignition delay times and laminar flame speed measurements [26,28] and flow reactors studies [23,25,29]. However, despite these efforts, there is still necessity of both, more accurate direct experimental determination of important rate constants and more experimental data to be used for validation and further improvement of modeling predictions [13,15].

In this context, this work addresses the conversion of CH_4/H_2S mixtures at different pressures, from atmospheric to 41 bar, analyzing the influence of temperature (500–1050 K) and for different oxygen concentrations, which results in different stoichiometry conditions, both global and/or individual for either CH_4 and H_2S. The study includes both experiments performed in two different tubular flow reactors, which have been used in different works [29–34], and a kinetic modeling study for analyzing the conversion of the CH_4/H_2S mixtures considered. These results would be useful for analyzing the conventional combustion of natural sour gas, but also for the combustion of biogas [19], the Claus process [35] or oxy-combustion of the sour gas [13–15,36].

2. Experimental methodology

The co-oxidation of CH_4 and H_2S was studied performing experiments in two different experimental set-ups. The experimental set-up 1 was used to perform the high-pressure CH_4/H_2S mixtures oxidation experiments and it has been previously described in detail elsewhere [e.g. 30]. Therefore, only a brief description of the main features is provided here. Reactants: H_2S, CH_4, O_2 and N_2 as carrier gas, were supplied from gas cylinders through mass flow controllers with an uncertainty in the flow rate measurements of approximately 0.5%. The reactant gases were premixed before entering the reactor, which consists of a quartz tube (inner diameter of 6 mm and 1500 mm in length) designed to approximate plug flow conditions [37]. The reactor is enclosed in a stainless-steel tube that acts as a pressure shell. The steel tube is placed horizontally in a tubular oven, with three individually controlled electrical heating elements that ensure an isothermal reaction zone of approximately 500 mm, with a uniform temperature profile (± 5 K). The total flow rate in all experiments has been 1 L (STP)/min. Gas residence time in the isothermal part of the reactor depends on pressure and temperature and it can be expressed as $t_r(s) = 232*P(bar)/T(K)$. Previously to the gas analysis systems, gases pass through a filter and a condenser to ensure gas cleaning. Products are analyzed by a gas micro-chromatograph (μGC) equipped with a thermal conductivity detector (TCD) calibrated to quantify H_2S, CH_4, O_2, CO, CO_2, C_2H_4, C_2H_6, CH_3SH and CS_2. A continuous UV analyzer was used to quantify SO_2. The uncertainty of the measurements is estimated within 5%.

The experiments carried out in this work using the set-up 1 correspond to sets 1–11 in Table 1. The experimental conditions for each set of experiments: manometric pressure, concentrations of reactants and corresponding air excess ratios used (λ, defined as inlet oxygen divided by stoichiometric oxygen) are specified. In order to calculate λ, the oxygen required for the complete oxidation of H_2S has been used (λ_{H2S}, according to reaction $H_2S + 1.5O_2 = SO_2 + H_2O$), for CH_4 (λ_{CH4}, according to reaction $CH_4 + 2O_2 = CO_2 + 2H_2O$) and for both together (λ_{total}). Stoichiometric and slightly fuel lean conditions ($\lambda_{total} \approx 1$) were selected to study the oxidation of CH_4/H_2S mixtures at high pressures, while stoichiometric and oxidizing conditions were used under near atmospheric pressures. Only an experiment for a $\lambda_{total} < 1$, set 9, was also done for the pressure of 20 bar, due to the potential deposition of sulfur species in the high-pressure experimental set-up under reducing conditions. The moderate concentration of oxygen used in this work was chosen to minimize SO_3 formation, which is enhanced at oxidizing conditions and high pressures and could lead to corrosion problems [38,39]. Stoichiometric and more oxidizing conditions were used under near atmospheric pressures (0.65 bar manometric pressure). Also different ratios between CH_4 and H_2S inlet concentrations were chosen for this pressure.

Additionally to the mixtures, selected experiments using only CH_4 (sets 10 and 11 in Table 1) or H_2S were performed for comparison. Experimental data for neat H_2S oxidation experiments (sets 12–15 in Table 1) were taken from another work of the authors carried out in the same high-pressure installation (set-up 1) [40].

A different set-up (set-up 2 in Table 1) was used in order to evaluate the oxidation of CH_4 and H_2S at atmospheric pressure. A detailed description of this set-up can be found in a recent work [41]. It consists of a tubular flow reactor in an electrically heated oven, with an isothermal reaction zone of 200 mm and 8.7 mm of internal diameter. The total flow rate in all experiments was 1 L (STP)/min, resulting in a gas residence time as a function of temperature of 194.6/T(K), in seconds. The oxidation experiments, sets 16–21 in Table 1, were performed at three different stoichiometries (reducing, stoichiometric and oxidizing conditions) in the temperature range of 700–1400 K, using a concentration of water vapour of 1%. In the process, the water vapour was used to minimize the effect, if any, of radical termination reactions on the walls of the reactor, which can be more important operating at atmospheric pressure. However, in this case, water vapour presence is not expected to have an influence on the present results, as reported in the work by Alzueta et al. [41] about CH_3SH oxidation in one of the reactors used here (set-up 2 in Table 1), where the effect of H_2O (0.5%) was evaluated. Additionally, an example of the results obtained in experiments for H_2S oxidation at atmospheric pressure, with and without water, in the set-up 2, is shown in Fig. S1 of the supplementary material. Since the differences between the results were negligible, we inferred that no significant effects of radical recombination on surface were occurring. The results obtained in the neat H_2S oxidation experiments, sets 22 and 23 in Table 1, have been taken from another work of the authors [29].

Table 1
Experimental conditions. N_2 as bath gas.

Set	Set-up	Residence time, t_r (s)	Manometric Pressure (bar)	[CH_4] (ppm)	[H_2S] (ppm)	[O_2] (ppm)	λ CH_4	λ H_2S	λ_{total}	Ref.
1	1	$232 \cdot \frac{P(bar)}{T(K)}$	0.65	1569	480	4500	1.43	6.25	1.17	p.w.
2	1	$232 \cdot \frac{P(bar)}{T(K)}$	0.65	–	525	4510	–	5.73	5.73	p.w.
3	1	$232 \cdot \frac{P(bar)}{T(K)}$	0.65	1350	1250	4590	1.70	2.45	1.00	p.w.
4	1	$232 \cdot \frac{P(bar)}{T(K)}$	0.65	1307	1255	25,500	9.76	13.5	5.67	p.w.
5	1	$232 \cdot \frac{P(bar)}{T(K)}$	0.65	480	1270	11,300	11.77	5.93	3.94	p.w.
6	1	$232 \cdot \frac{P(bar)}{T(K)}$	10	1282	1243	4550	1.77	2.44	1.03	p.w.
7	1	$232 \cdot \frac{P(bar)}{T(K)}$	20	1303	1224	4503	1.73	2.45	1.01	p.w.
8	1	$232 \cdot \frac{P(bar)}{T(K)}$	40	1320	1230	4600	1.74	2.49	1.03	p.w.
9	1	$232 \cdot \frac{P(bar)}{T(K)}$	20	1315	1295	1804	0.68	0.93	0.39	p.w.
10	1	$232 \cdot \frac{P(bar)}{T(K)}$	20	1348	–	4286	1.59	–	1.59	p.w.
11	1	$232 \cdot \frac{P(bar)}{T(K)}$	40	1400	–	4500	1.61	–	1.61	p.w.
12	1	$232 \cdot \frac{P(bar)}{T(K)}$	0.65	–	505	1509	–	1.99	1.99	[40]
13	1	$232 \cdot \frac{P(bar)}{T(K)}$	10	–	485	1510	–	2.06	2.06	[40]
14	1	$232 \cdot \frac{P(bar)}{T(K)}$	20	–	497	1520	–	2.04	2.04	[40]
15	1	$232 \cdot \frac{P(bar)}{T(K)}$	40	–	500	1545	–	2.06	2.06	[40]
16	2	$\frac{194.6}{T(K)}$	Atmospheric	1517	–	750	0.25	–	0.25	p.w.
17	2	$\frac{194.6}{T(K)}$	Atmospheric	1517	–	3000	0.99	–	0.99	p.w.
18	2	$\frac{194.6}{T(K)}$	Atmospheric	1508	–	6000	1.99	–	1.99	p.w.
19	2	$\frac{194.6}{T(K)}$	Atmospheric	1510	279	750	0.25	1.79	0.22	p.w.
20	2	$\frac{194.6}{T(K)}$	Atmospheric	1513	285	3000	0.99	7.02	0.87	p.w.
21	2	$\frac{194.6}{T(K)}$	Atmospheric	1508	298	6000	1.99	13.4	1.73	p.w.
22	2	$\frac{194.6}{T(K)}$	Atmospheric	–	482	1500	–	2.07	2.07	[29]
23	2	$\frac{194.6}{T(K)}$	Atmospheric	–	492	3750	–	5.08	5.08	[29]

p.w. denotes present work.

3. Kinetic model

The kinetic model used in the present study is based on previous works from the authors, and it counts with reactions related to the interaction of carbon and sulfur species from the work of Alzueta et al. [42], about the inhibition and sensitization of fuel (CO) oxidation by SO_2. It also considers another study about CS_2 and COS conversion under different combustion conditions [43], and the work from Abián et al. [44] where the impact of the presence of SO_2 on the formation of soot from ethylene pyrolysis was evaluated. The description of H_2S conversion is taken from the work by Colom-Díaz et al. [29], counting with an updated subset of H_2S reactions, mainly based on the work from Zhou et al. [27] and Song et al. [25].

Besides, the present mechanism has been updated with some reactions from recent studies. For example, the H_2/O_2 reaction subset, which is important for the radical pool composition, has been taken from the examination at high pressures of H_2 oxidation and its interaction with NO [34]. New subsets have been added from the study of Gersen et al. [23], about CH_4/H_2S oxidation at high pressures, where the peroxides CH_3OO and CH_3OOH chemistry was found to be important at high pressures and low temperatures, based on previous studies from the same group about CH_4 oxidation at high pressures [24,45]. Thus, CH_3OO and CH_3OOH reaction subsets have been added. The formation and consumption of organosulfur compounds like CH_3SH were also found important in [23], and a subset describing CH_3SH conversion taken from the work of Alzueta et al. [41], which was based on the works of Zheng et al. [46] and Van de Vijver et al. [47], has been included. As for thermochemical data, same sources as for the corresponding reactions were used. Kinetic calculations were carried out in the frame of Chemkin Pro with the PFR model [48]. Ultimately, some key reactions have been updated, which are described in detail in

the next section. The mechanism listing can be found as supplementary material.

4. Results and discussion

The experimental results of H_2S, SO_2, CH_4 and CO concentrations corresponding to the experiments near atmospheric pressure (set-up 1), sets 1–5 and 12 from Table 1, are presented from Figs. 1–4 together with the kinetic modelling predictions (lines). The species CO_2, C_2H_4, C_2H_6, CH_3SH and CS_2 were detected in small concentrations and, therefore, they are not shown in the figures. In all figures, symbols represent experimental concentrations, while lines denote model predictions. Additional graphics with normalized H_2S and CH_4 concentrations have been included in the supplementary material to facilitate the poste-
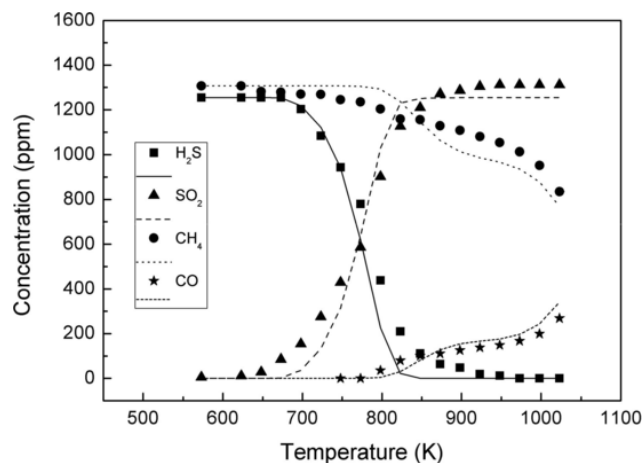

Fig. 1. Concentrations of H_2S, SO_2, CH_4 and CO vs. temperature at the experimental conditions of set 4 in Table 1 (λ_{total} = 5.67), 0.65 bar.
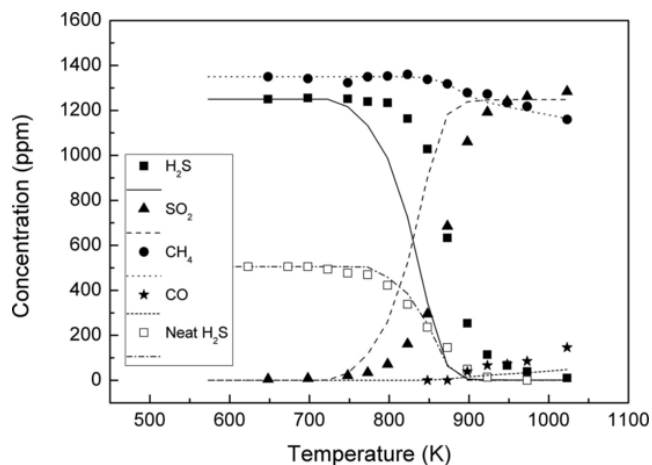
Fig. 2. Concentrations of H_2S, SO_2, CH_4 and CO vs. temperature at the experimental conditions of sets 3 ($\lambda_{total} = 1.00$) and 12 ($\lambda_{total} = 1.99$) in Table 1, 0.65 bar.

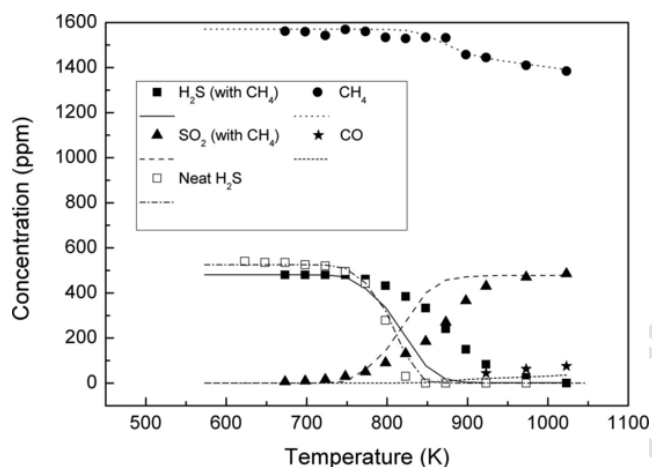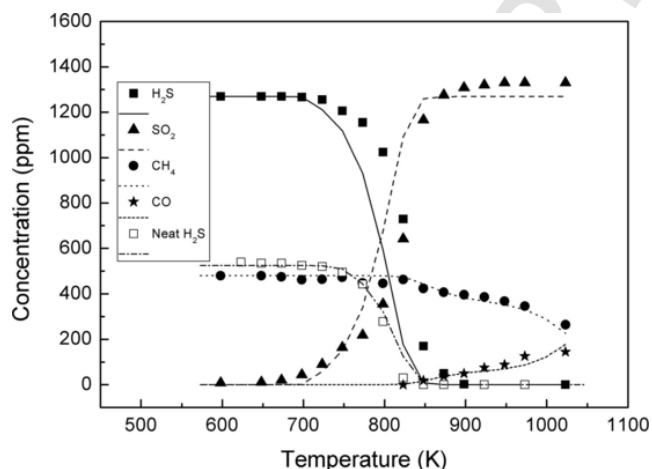**Fig. 3.** Concentrations of H_2S, SO_2, CH_4 and CO vs. temperature at the experimental conditions of set 1 ($\lambda_{total} = 1.17$) and 2 ($\lambda_{total} = 5.73$) in Table 1, 0.65 bar.

Fig. 4. Concentrations of H_2S, SO_2, CH_4 and CO vs. temperature at the experimental conditions of sets 5 ($\lambda_{total} = 3.94$) and 2 ($\lambda_{total} = 5.73$) in Table 1, 0.65 bar.

rior discussion (Figs. S2 and S3) on the effect of λ and pressure in the results. Different stoichiometry values and CH_4/H_2S ratios have been used to study the oxidation behaviour of the CH_4/H_2S mixtures near atmospheric pressure. The experimental results using oxidizing conditions (set 4, $\lambda_{total} = 5.67$) are shown in Fig. 1. H_2S oxidation occurs

at temperatures lower than the ones at which CH_4 oxidation occurs, being H_2S completely converted into SO_2 at temperatures above approximately 900 K. The experimental trends are fairly well captured by the mechanism. It is remarkable that the oxidation of hydrogen sulfide occurs similarly to the results obtained in a work at atmospheric pressure in a different flow reactor (set-up 2) when studying the conversion of neat H_2S at atmospheric pressure [29]. The consumption of H_2S is due to its reactions with H and HO_2 radicals (R1 and R2). The radical SH formed further reacts with oxygen to form the peroxide HSOO (R3), which isomerizes to HSO_2 (R4) and, then, forms $SO_2 + H$ via (R5) or reacts with O_2, due to the high concentration available, to form $SO_2 + HO_2$ (R6).

$$H_2S + H \rightleftharpoons SH + H_2 \tag{R1}$$

$$H_2S + HO_2 \rightleftharpoons SH + H_2O_2 \tag{R2}$$

$$SH + O_2(+M) \rightleftharpoons HSOO(+M) \tag{R3}$$

$$HSOO \rightleftharpoons HSO_2 \tag{R4}$$

$$HSO_2(+M) \rightleftharpoons SO_2 + H(+M) \tag{R5}$$

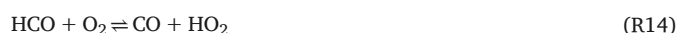$$HSO_2 + O_2 \rightleftharpoons SO_2 + HO_2 \tag{R6}$$

The oxidation of methane in the CH_4/H_2S mixture occurs at lower temperatures compared to the oxidation of neat methane, due to the radicals coming from H_2S oxidation. Regarding neat CH_4, it did not show any reactivity in the simulation runs in these conditions. Methane reacts with OH radicals to form CH_3 (R7), which, depending on the temperature, will form different products.

$$CH_4 + OH \rightleftharpoons CH_3 + H_2O \tag{R7}$$

At low temperatures (850 K), CH_3 forms mainly CH_3O (R8) and C_2H_6 (R9), while at higher temperatures the reaction with O_2 to form CH_2O is predominant (R10). CH_3 also reacts with HO_2 to regenerate CH_4 via (R11), being less important as the temperature increases.

$$CH_3 + HO_2 \rightleftharpoons CH_3O + OH \tag{R8}$$

$$CH_3 + CH_3(+M) \rightleftharpoons C_2H_6(+M) \tag{R9}$$

$$CH_3 + O_2 \rightleftharpoons CH_2O + OH \tag{R10}$$

$$CH_3 + HO_2 \rightleftharpoons CH_4 + O_2 \tag{R11}$$

The oxidation continues with CH_3O species decomposing to $CH_2O + H$ (R12) and proceeding to CO via (R13) and (R14). The pathway leading to C_2H_6 might continue with its reaction to C_2H_5 (R15) and C_2H_4 (R16) later on. The oxidation behavior of methane is similar to that presented in the work of Giménez-López et al. [49] about oxy-fuel oxidation of methane.

$$CH_3O(+M) \rightleftharpoons CH_2O + H(+M) \tag{R12}$$

$$CH_2O + OH \rightleftharpoons HCO + H_2O \tag{R13}$$

$$HCO + O_2 \rightleftharpoons CO + HO_2 \tag{R14}$$

$$C_2H_6 + OH \rightleftharpoons C_2H_5 + H_2O \tag{R15}$$

$$C_2H_5 + O_2 \rightleftharpoons C_2H_4 + HO_2 \tag{R16}$$

The oxidation of both species (CH_4 and H_2S) occurs separately at a high concentration of O_2; i.e. when H_2S is fully consumed, CH_4 conversion increases coinciding with a higher formation of CO, and no presence of C-S species is detected. However, if the oxygen concentration is reduced, the oxidation behavior changes. The experimental trends of the oxidation of CH_4/H_2S mixtures at stoichiometric conditions ($\lambda_{total} = 1.00$, $\lambda_{CH4} = 1.70$, $\lambda_{H2S} = 2.45$) (set 3 in Table 1) are presented

in Fig. 2, together with its comparison with neat H_2S oxidation (set 12 in Table 1), using around the same λ_{H2S} value. It is shown that methane oxidation is still promoted to lower temperatures, but to a lower extent compared to the case of oxidizing conditions. In the case of H_2S, its consumption is shifted to higher temperatures (by 75 K) compared to the neat oxidation of H_2S, indicating therefore the different behavior of H_2S conversion when studying neat oxidation of H_2S or in the CH_4/H_2S mixture. A similar case can be observed in the study of Zeng et al. [50], about the co-oxidation of CH_4 and CS_2 in a flow reactor, where they also saw experimentally a delay in the oxidation of CS_2 by CH_4 and that trace amounts of CS_2 reduce the ignition temperature of CH_4. The authors indicated that the C-H-O-S combustion chemistry was complex and consequently their mechanism could not include all potential reactions. In our case, the kinetic model cannot predict the inhibition of H_2S conversion by CH_4 to higher temperatures either, despite the inclusion in the present mechanism of the CH_3SH, CS_2 and COS conversion subsets.

With the aim of improving this situation, reaction (R17) has been also updated with the value for its kinetic constant recommended by Zeng et al. [51], who revised this reaction using the CBS-QB3 level of theory, mentioning that it was overestimated before at lower temperatures.

$$CH_3 + H_2S \rightleftharpoons CH_4 + SH \qquad (R17)$$

This change has produced improvements in model predictions for the CH_4 oxidation at all conditions studied. Also new reactions (R18) and (R19) from the work of Zeng et al. [51] have been added, but they are not important under the experimental conditions considered.

$$CH_4 + S_2 \rightleftharpoons CH_3 + HS_2 \qquad (R18)$$

$$CH_4 + SO \rightleftharpoons CH_3 + HSO \qquad (R19)$$

Fig. 3 shows the results of the conversion of the CH_4/H_2S mixture (set 1 in Table 1) and neat H_2S (set 2 in Table 1) for similar inlet concentrations of H_2S and O_2, i.e. similar values of λ_{H2S}. In this manner, we can analyze if for $\lambda_{H2S} \approx 6$, CH_4 still has the potential to inhibit the oxidation of H_2S or the O_2 will oxidize completely the H_2S, as in the case of Fig. 1. As can be observed in Fig. 3, there is still a shift of the H_2S conversion to higher temperatures in the presence of CH_4 in comparison with the case of neat H_2S. While the conversion of neat H_2S and the neat CH_4 oxidation are well captured by the model, simulations are shifted at lower temperatures for H_2S in the mixture oxidation.

It is also interesting to compare the results obtained in set 3 (Fig. 2) and set 1 (Fig. 3) corresponding to similar λ_{CH4} and λ_{total}, but different H_2S inlet concentrations (1250 and 480 ppm, respectively) and CH_4/H_2S ratios (1.1 and 3.2, respectively). It can be observed that the onset of H_2S conversion in set 1 (Fig. 3) occurs at lower temperature than that obtained in set 3 (Fig. 2), due to the higher λ_{H2S} in set 1. On the other hand, by comparison with set 3, the conversion of H_2S in set 1 finishes at higher temperatures, which might be due to the higher CH_4/H_2S ratio in set 1 (i.e. more CH_4 consuming necessary radicals for H_2S oxidation). This can also be clearly observed in Fig. S2 of the supplementary material.

If the CH_4/H_2S ratio is reduced, Fig. 4, using the same λ_{H2S} as in Fig. 3 ($\lambda_{H2S} \approx 6$), we can evaluate if a comparatively lower concentration of methane will decrease the inhibition process. As it is shown, the H_2S oxidation finishes at lower temperatures in comparison with the results shown in Fig. 3 (see also Fig. S2 of the supplementary material), where a higher concentration of CH_4 was used, hence, consuming more radicals needed for the conversion of H_2S. However, we cannot assure if the delay in the ignition temperature of H_2S, in comparison with neat H_2S, is due to the consumption of radicals from the radical pool by CH_4, or due to the formation of some carbon-sulfur intermediate species, even though they were not detected in the μGC analysis.

It is worth to mention that, except in the case of oxidizing conditions (Fig. 1), in each of the Figs. 2-4 a weak minimum in CH_4 concentration during the oxidation of H_2S can be observed at low temperatures, which could indicate some interaction somehow during the conversion of the mixtures. Additionally, as mentioned by Mulvihill et al. [28] about the importance of C-S species in process modeling, Gersen et al. [23] included C-S species in their mechanism, while Bongartz and Ghoniem [14] excluded them, obtaining both of them predictions with their models nearly similar for all shock-tube experiments. It is suggested, then, that this similarity in predictions between the two mechanisms could indicate that these C-S species are unimportant at shock-tube conditions, while the work from Mulvihill et al. [28] about flame speeds showed 4 reactions involving C-S species within the most sensitive ones. Thus, depending on the experimental conditions, C-S species might take a significant role in the oxidation process.

As the pressure increases, the conversion of both CH_4 and H_2S in the oxidation of CH_4/H_2S mixtures is shifted to lower temperatures. The concentrations of H_2S, SO_2, CH_4 and CO, as a function of temperature, at 10, 20 and 40 bar, using stoichiometric conditions (λ_{total} near 1) for CH_4/H_2S mixtures, are plotted in Figs. 5-7. Results obtained for oxidation of neat H_2S ($\lambda_{total} \approx 2$) are also shown. In the case of 20 and 40 bar, the oxidation of neat CH_4 ($\lambda_{total} \approx 1.6$) is also included, since these are the only cases in which neat methane was found to be reactive, in the temperature range studied.
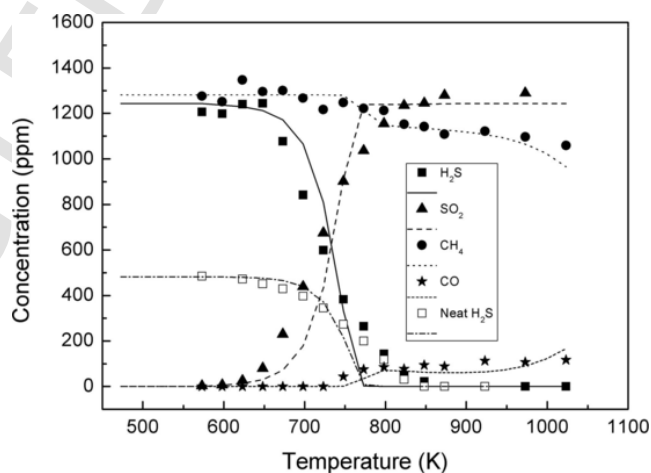

Fig. 5. Concentrations of H_2S, SO_2, CH_4 and CO vs. temperature at the experimental conditions of sets 6 ($\lambda_{total} = 1.03$) and 13 ($\lambda_{total} = 2.06$) in Table 1, 10 bar.
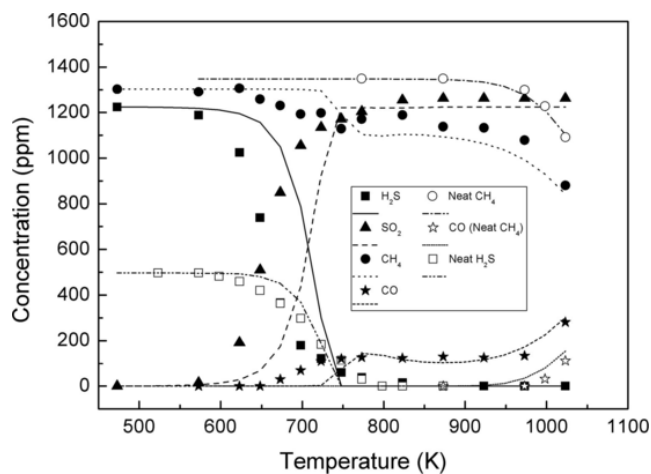

Fig. 6. Concentrations of H_2S, SO_2, CH_4 and CO vs. temperature at the experimental conditions of sets 7 ($\lambda_{total} = 1.01$), 10 ($\lambda_{total} = 1.59$) and 14 ($\lambda_{total} = 2.04$) in Table 1, 20 bar.
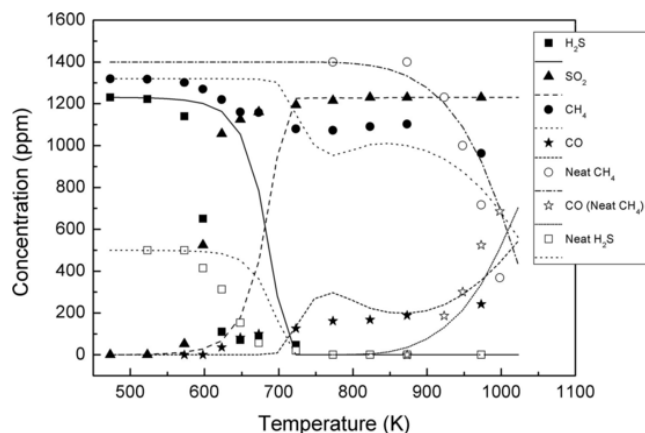
Fig. 7. Concentrations of H_2S, SO_2, CH_4 and CO vs. temperature at the experimental conditions of sets 8 ($\lambda_{total} = 1.03$), 11 ($\lambda_{total} = 1.61$) and 15 ($\lambda_{total} = 2.06$) in Table 1, 40 bar.

The conversion of CH_4 is seen to occur and, as the conversion of H_2S, it is shifted to lower temperatures as the pressure increases. The effect of the pressure at stoichiometric conditions for CH_4/H_2S oxidation ($\lambda \approx 1$, sets 3, 6, 7 and 8 in Table 1) can be observed in Fig. S3 of the supplementary material. In the case of 10 bar, the oxidation of H_2S is almost the same with and without CH_4, whereas at 20 and 40 bar, H_2S is even slightly promoted. The oxidation trend of CH_4 is still fairly well captured by the model, in the case of the neat CH_4 and co-oxidation. The biggest differences between modeling results and experimental concentrations are found in H_2S conversion at 40 bar, which are the same differences for neat H_2S as in the presence of CH_4. Thus, this could be attributed to the present description of the H_2S chemistry at high pressure [40].

According to the model calculations, H_2S conversion starts via (R20), as was also mentioned by Gersen et al. [23]. In the same way, Zhou et al. [27] mentioned the sensitivity of (R20) in their model due to the role to determine the ignition temperature of H_2S.
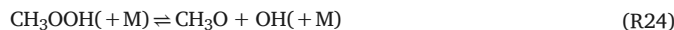
$$H_2S + O_2 \rightleftharpoons SH + HO_2 \tag{R20}$$

Once conversion is started, the consumption of H_2S is mainly maintained through reaction of H_2S with HO_2 radicals (R2), radicals which formation is enhanced at high pressures [e.g. 23,25,26]. At the same time, H_2O_2 formation (R2), also favored at high pressures, promotes the reaction via the branching reaction (R21). The conversion of H_2S follows, as mentioned before, with (R3) and (R4), with (R6) as the main final step.

$$H_2O_2(+M) \rightleftharpoons OH + OH(+M) \tag{R21}$$

The conversion of CH_4 in the mixture is influenced by H_2S oxidation, being the influence more noticeable as pressure increases, reaching 20% of conversion between 700 and 900 K at 40 bar. H_2S oxidation provides radicals to the radical pool and, at the same time, higher pressures involve a major role of peroxides like CH_3OO and HO_2 in the oxidation process of CH_4. At high pressures, other pathways become important in comparison with the previous ones mentioned near atmospheric pressure. Depending on temperature, the model predicts that CH_4 consumption is dependent on the reactions of CH_3 to form different products. At intermediate temperatures and high pressures, formation of peroxyl radicals may be significant [e.g. 24,32,33]. Actually, at low temperatures and high pressures (e.g. 725 K at 40 bar), the formation of the peroxide CH_3OO is the preferred channel (R22),

$$CH_3 + O_2 \rightleftharpoons CH_3OO \tag{R22}$$

which will continue reacting through (R23), (R24), (R12), (R13) and (R14), and finally decomposed to CO in the final step (R25).

$$CH_3OO + HO_2 \rightleftharpoons CH_3OOH + O_2 \tag{R23}$$

$$CH_3OOH(+M) \rightleftharpoons CH_3O + OH(+M) \tag{R24}$$

$$HCO + M \rightleftharpoons H + CO + M \tag{R25}$$

As temperature rises, other pathways become important. At 800 K and 40 bar, radical CH_3 reacts with HO_2 radicals to give CH_3O (R8), instead of producing only CH_3OO, which also ends up as CH_3O, being the net result of the CH_3OO pathway similar to reaction (R8). CH_3O decomposes thermally to CH_2O, as mentioned before via (R12), and ends as CO through (R13), (R14) and (R25). The pathway to produce C_2H_6 also becomes important at this temperature (R9). From 900 K and above, the branching ratio shifts toward the production of CH_2O (R10) from CH_3, which is the main pathway for neat CH_4 oxidation as well. CH_2O can react with HO_2 radicals too (R26), as well as with CH_3 to regenerate CH_4 (R27), like reaction (R28), but mainly CH_2O reacts with OH radicals (R13).

$$CH_2O + HO_2 \rightleftharpoons HCO + H_2O_2 \tag{R26}$$

$$CH_2O + CH_3 \rightleftharpoons HCO + CH_4 \tag{R27}$$

$$CH_3 + H_2 \rightleftharpoons CH_4 + H \tag{R28}$$

Regarding reaction R10 ($CH_3 + O_2 \rightleftharpoons CH_2O + OH$), we found large discrepancies in our modeling results using different kinetic parameters from the literature. This reaction has been broadly discussed over the years, as it is important for the combustion of hydrocarbons, since it exists a competition with reaction (R29) at high temperatures and with (R22) at low temperatures.

$$CH_3 + O_2 \rightleftharpoons CH_3O + O \tag{R29}$$

It is difficult to determine the product branching ratios quantitatively for the two high temperature competitive reaction channels (R10 and R29), because the reactions are slow and only high-temperature measurements, above approximately 1300 K, behind shock waves could produce some meaningful data [52]. A large scatter in the rate coefficients determined over the years for the $CH_3 + O_2$ reaction system exists. In the case of the works of Glarborǵs group involving CH_4 oxidation at high pressures [23,24,45,53], they use the kinetic parameters from Srinivasan et al. [54], who combined their own measurements with literature data [55–57] across the temperature range 1237–2430 K. In our simulations, these kinetic parameters are too fast for neat CH_4 conversion, which are out of the temperature range considered in the present work. Although, as mentioned by Fernandes et al. [58], this problem seemed to have been settled by Herbon et al. [57] and Srinivasan et al. [54], whose determinations for these reactions were in near agreement with the theoretical modelling results from Zhu et al. [52]. Srinivasan et al. reviewed this reaction (R10) in 2007 providing new experiments in a shock tube over the temperature range 1224–1502 K, and yielding an updated kinetic expression [59].

Other recent studies including subsets for CH_4 conversion in their mechanisms, such as the works of Alzueta et al. [41] and Marrodán et al. [32,33], used the expression of Yu et al. [55], but these values appear to be too slow to describe the neat oxidation of CH_4 under the current experimental conditions. Also, the parameters proposed by Fernandes et al. [58] have been used in different woks [e.g. 15,60,61], but those appear to be too low to reproduce our experimental results.

Hence, the authors have decided to use for (R10) the revisited parameters proposed from Srinivasan et al. [59]. As seen in Fig. 8, the kinetic constant values chosen fall just between the kinetic parameters lastly used in the literature in high pressures studies [54] and [58], and it is near the recommendation from Baulch et al. [62]. We think that this might be a reasonable estimation for the temperature
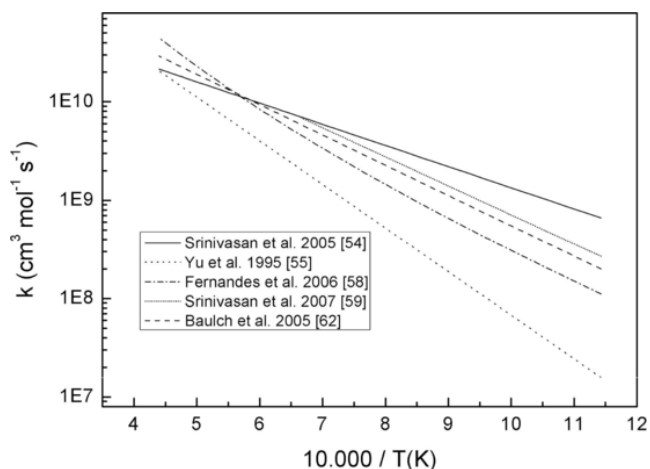
Fig. 8. Kinetic constant for reaction $CH_3 + O_2 = CH_2O + OH$ (R10) using kinetic parameters from the literature as a function of temperature, $1 \cdot 10^4/T(K)$.

range studied in this work, which falls out of the ones usually used to determine it (R10).

The experimental results for the experiment at reducing conditions ($\lambda_{total} = 0.39$) at 20 bar (set 9 in Table 1) are shown in Fig. 9. The carbon and sulphur balances remain near 100% at all temperatures (around 5%) and no C-S species were found in the analysis. H_2S conversion is more gradual than in the case near stoichiometric conditions at 20 bar, which cannot be predicted by the model. Methane concentration presents two slight minimums and is almost unreactive all across the temperature range considered.

In addition, the results obtained in the experiments of the CH_4/H_2S co-oxidation in the atmospheric pressure set-up (set-up 2) are shown in Figs. 10–12. As it can be observed, the trends are similar to the ones found in the high-pressure reactor (set-up 1) under near atmospheric pressure conditions. CH_4 oxidation is shifted to lower temperatures due to the presence of H_2S at all conditions considered. In the case of H_2S oxidation, its conversion is shifted to higher temperatures in the presence of CH_4, and a more gradual behaviour is seen at all conditions. The CH_4 onset temperature is different from one reactor to another. If the experiments at stoichiometric conditions are compared, there is a difference of 200 K (900 K at the set-up 1 and 1100 K at the set-up 2). This is attributed to the difference in gas residence times, as the gas residence time in the high pressure reactor (set-up 1) working near atmospheric pressure doubles the one in the reactor at atmospheric pressure (set-up 2). The kinetic model captures fairly well the oxida-
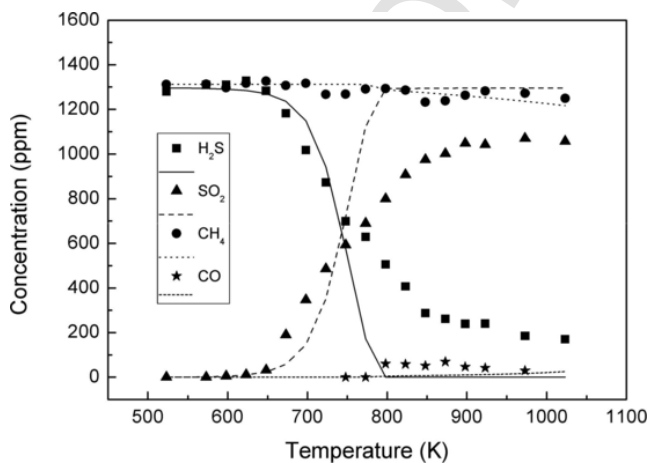

Fig. 10. Concentrations of H_2S, SO_2, CH_4 and CO vs. temperature at the experimental conditions of sets 16 ($\lambda_{total} = 0.25$), 19 ($\lambda_{total} = 0.22$) and 22 ($\lambda_{total} = 2.07$) in Table 1, atmospheric pressure.

Fig. 11. Concentrations of H_2S, SO_2, CH_4 and CO vs. temperature at the experimental conditions of sets 17 ($\lambda_{total} = 0.99$), 20 ($\lambda_{total} = 0.87$) and 23 ($\lambda_{total} = 5.08$) in Table 1, atmospheric pressure.

Fig. 9. Concentrations of H_2S, SO_2, CH_4 and CO vs. temperature at the experimental conditions of set 9 ($\lambda_{total} = 0.39$) in Table 1, 20 bar.
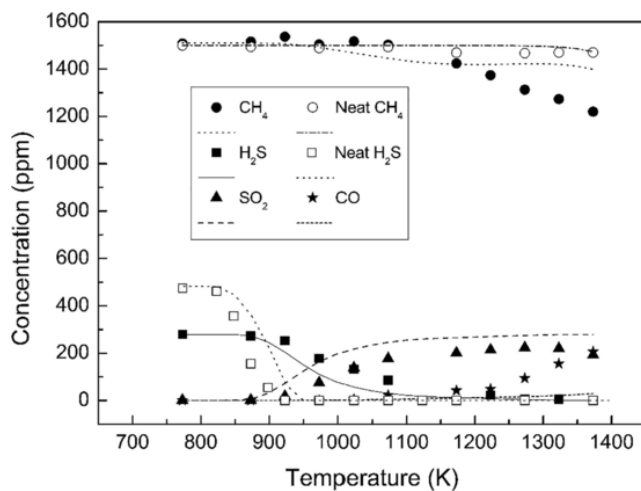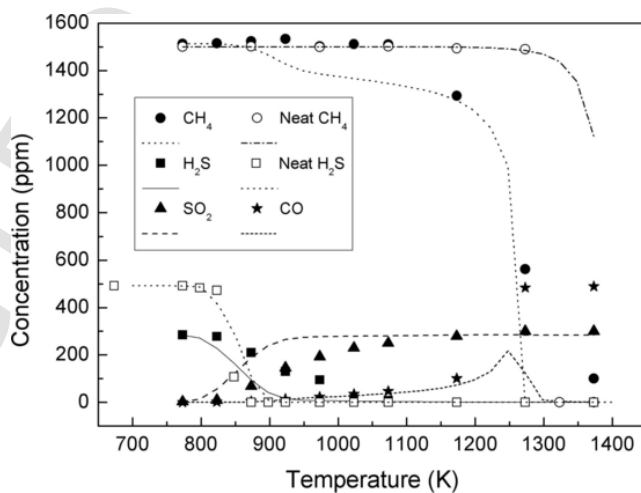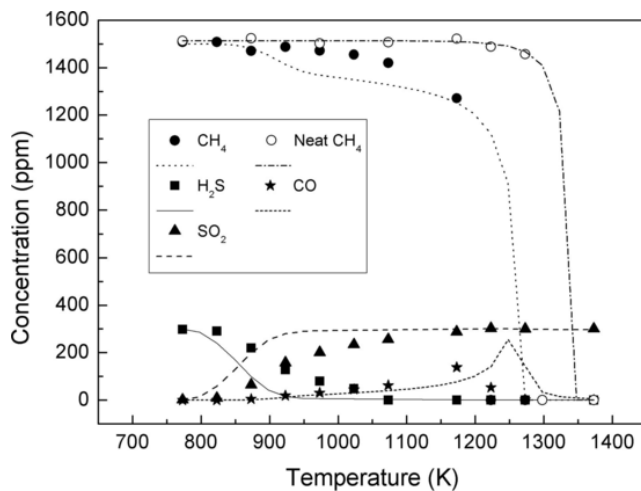

Fig. 12. Concentrations of H_2S, SO_2, CH_4 and CO vs. temperature at the experimental conditions of sets 18 ($\lambda_{total} = 1.99$) and 21 ($\lambda_{total} = 1.73$) in Table 1, atmospheric pressure.

tion trends. However, it overpredicts the oxidation of H_2S and CH_4 by a small margin, except at reducing conditions, where CH_4 oxidation is not captured at high temperatures.

5. Conclusions

The oxidation of CH_4/H_2S mixtures in two different flow reactor set-ups, at different pressures, CH_4/H_2S ratios and stoichiometries, in the temperature range of 500–1400 K, has been studied. The oxidation of both CH_4 and H_2S in the mixtures is shifted to lower temperatures as pressure increases. H_2S promotes CH_4 oxidation to lower temperatures. The presence of CH_4 inhibits the oxidation of H_2S under near atmospheric pressure, being this inhibition less important at higher pressures. A kinetic model based on published literature mechanisms has been further updated in order to reproduce the experimental results over a wide range of conditions. The kinetic model here used seems to predict fairly well the trend of CH_4 and H_2S evolution at almost all conditions considered. However, in the case of H_2S, the model does not capture accurately the experimental results under near atmospheric pressure and 40 bar, which might be related to H_2S conversion chemistry. The results obtained in this work, as well as the kinetic model used, might be useful for practical purposes dealing with both combustion or chemical processes, such as the Claus process.

Declaration of Competing Interest

The authors declare that they have no known competing financial interests or personal relationships that could have appeared to influence the work reported in this paper.

Acknowledgements

Appendix A. Supplementary data

Supplementary data to this article can be found online at https://doi.org/10.1016/j.fuel.2019.116484.

References

[1] IEA International Energy Agency, World Energy Outlook, 2017.

[2] W Taifan, J Baltrusaitis. Minireview: direct catalytic conversion of sour natural gas (CH_4 + H_2S + CO_2) components to high value chemicals and fuels. Catal Sci Technol 2017;7:2919–2929.

[3] MA Mac Kinnon, J Brouwer, S Samuelsen. The role of natural gas and its infrastructure in mitigating greenhouse gas emissions, improving regional air quality, and renewable resource integration. Prog Energy Combust Sci 2018;64:62–92.

[4] Hammer G, Lübcke T, Kettner R, Pillarella MR, Recknagel H, Commichau A, Neumann H-J, Paczynska-Lahme B. Ullmann's Encyclopedia of Industrial Chemistry, Wiley-VCH: Weinheim, Germany, 2012, Vol. 23; Chapter Natural Gas, 739–92.

[5] US Department of Energy, Report of basic research needs for clean and efficient combustion of 21st century transportation fuels, 2006.

[6] I Salisu, KR Ramees, R Abhijeet. Dual-stage acid gas combustion to increase sulfur recovery and decrease the number of catalytic units in sulfur recovery units. Appl Therm Eng 2019;156:576–586.

[7] S Zarei, H Ganji, M Sadi, M Rashidzadeh. Thermo-kinetic modeling and optimization of the sulfur recovery unit thermal stage. Appl Therm Eng 2016;103:1095–1104.

[8] I Salisu, KR Ramees, R Abhijeet. Roles of hydrogen sulfide concentration and fuel gas injection on aromatics emission from Claus furnace. Chem Eng Sci 2017;172:513–527.

[9] Rameshni M. Cost effective options to expand SRU capacity using oxygen, Sulfur Recovery Symposium Brimstone Engineering Services, Inc Banlf, Alberta, Calgary Alberta, Calgary, May 2002.

[10] D Barba, F Cammarota, V Vaiano, E Salzano, V Palma. Experimental and numerical analysis of the oxidative decomposition of H_2S. Fuel 2017;198:68–75.

[11] I Salisu, R Abhijeet. Kinetic simulation of acid gas (H_2S and CO_2) destruction for simultaneous syngas and sulfur recovery. Ind Eng Chem Res 2016;55:6743–6752.

[12] Rameshni M, Santo S. Production of elemental sulphur from SO2 (RSR). 2006 TMS Fall Extraction and Processing Division: Sohn International Symposium. 8. 469–488.

[13] D Bongartz, SJ Shanbhogue, AF Ghoniem. Formation and control of sulfur oxides in sour gas oxy-combustion: prediction using a reactor network model. Energy Fuels 2015;29:7670–7680.

[14] D Bongartz, AF Ghoniem. Impact of sour gas composition on ignition delay and burning velocity in air and oxy-fuel combustion. Combust Flame 2015;162:2749–2757.

[15] D Bongartz, AF Ghoniem. Chemical kinetics mechanism for oxy-fuel combustion of mixtures of hydrogen sulfide and methane. Combust Flame 2015;162:544–553.

[16] A Gopan, BM Kumfer, RL Axelbaum. Effect of operating pressure and fuel moisture on net plant efficiency of a staged, pressurized oxy-combustion power plant. Int J Greenhouse Gas Control 2015;39:390–396.

[17] X Wang, A Adeosun, G Yablonsky, A Gopan, P Du, RL Axelbaum. Synergistic SO_x/NO_x chemistry leading to enhanced SO_3 and NO_2 formation during pressurized oxy-combustion. React Kinet Mech Catal 2018;123:313–322.

[18] O Awe, Y Zhao, A Nzihou, D Minh, N Lyczko. A review of biogas utilisation, purification and upgrading technologies. Waste Biomass Valor 2017;8:267–283.

[19] A Valera-Medina, A Giles, D Pugh, S Morris, M Pohl, A Ortwein. Investigation of combustion of emulated biogas in a gas turbine test rig. J Therm Sci 2018;27:331–340.

[20] W Jerzak, M Kuźnia, A Szajding. Experimental studies and the chemical kinetics modelling of oxidation of hydrogen sulfide contained in biogas. Procedia Eng 2016;157:222–229.

[21] HSF Chin, K Karan, AK Mehrotra, LA Behie. The fate of methane in a Claus plant reaction furnace. Can J Chem Eng 2001;79:482–490.

[22] K Karan, LA Behie. CS_2 formation in the Claus reaction furnace: a kinetic study of methane-sulfur and methane-hydrogen sulfide reactions. Ind Eng Chem Res 2004;43:3304–3313.

[23] S Gersen, M Van Essen, H Darmeveil, H Hashemi, CT Rasmussen, JM Christensen, et al. Experimental and modeling investigation of the effect of H_2S addition to methane on the ignition and oxidation at high pressures. Energy Fuels 2017;31:2175–2182.

[24] H Hashemi, JM Christensen, S Gersen, HB Levinsky, SJ Klippenstein, P Glarborg. High pressure oxidation of methane. Combust Flame 2016;172:349–364.

[25] Y Song, H Hashemi, JM Christensen, C Zou, BS Haynes, P Marshall, et al. An exploratory flow reactor study of H_2S oxidation at 30–100 bar. Int J Chem Kinet 2017;49:37–52.

[26] O Mathieu, F Deguillaume, EL Petersen. Effects of H_2S addition on hydrogen ignition behind reflected shock waves: experiments and modeling. Combust Flame 2014;161:23–36.

[27] CR Zhou, K Sendt, BS Haynes. Experimental and kinetic modelling study of H_2S oxidation. Proc Combust Inst 2013;34:625–632.

[28] CR Mulvihill, CL Keesee, T Sikes, RS Teixeira, O Mathieu, EL Petersen. Ignition delay times, laminar flame speeds, and species time-histories in the H_2S/CH_4 system at atmospheric pressure. Proc Combust Inst 2019;37:735–742.

[29] JM Colom-Díaz, M Abián, MY Ballester, Á Millera, R Bilbao, MU Alzueta. H_2S conversion in a tubular flow reactor: Experiments and kinetic modeling. Proc Combust Inst 2019;37:727–734.

[30] L Marrodán, Á Millera, R Bilbao, MU Alzueta. High-pressure study of methylformate oxidation and its interaction with NO. Energy Fuels 2014;28:6107–6115.

[31] L Marrodán, E Royo, Á Millera, R Bilbao, MU Alzueta. High-pressure oxidation of dimethoxymethane. Energy Fuels 2015;29:3507–3517.

[32] L Marrodán, AJ Arnal, Á Millera, R Bilbao, MU Alzueta. The inhibiting effect of NO addition on dimethyl ether high-pressure oxidation. Combust Flame 2018;197:1–10.

[33] L Marrodán, M Fuster, Á Millera, R Bilbao, MU Alzueta. Ethanol as a fuel additive: high-pressure oxidation of its mixtures with acetylene. Energy Fuels 2018;32:10078–10087.

[34] JM Colom-Díaz, Á Millera, R Bilbao, MU Alzueta. High pressure study of H_2 oxidation and its interaction with NO. Int J Hydrog Energy 2019;44:6325–6332.

[35] BS Haynes. Combustion research for chemical processing. Proc Combust Inst 2019;37:1–32.

[36] MB Toftegaard, J Brix, PA Jensen, P Glarborg, AD Jensen. Oxy fuel combustion of solid fuels. Prog Energy Combust Sci 2010;36:581–625.

[37] CL Rasmussen, J Hansen, P Marshall, P Glarborg. Experimental measurements and kinetic modeling of $CO/H_2/O_2/NO_x$ conversion at high pressure. Int J Chem Kinet 2008;40:454–580.

[38] JM Colom, MU Alzueta, JM Christensen, P Glarborg, R Cordtz, J Schramm. Importance of vanadium-catalyzed oxidation of SO_2 to SO_3 in two-stroke marine diesel engines. Energy Fuels 2016;30:6098–6102.

[39] D Fleig, MU Alzueta, F Normann, M Abián, K Andersson, F Johnsson. Combust Flame 2013;160:1142–1151.

[40] JM Colom-Díaz, M Abián, Á Millera, R Bilbao, MU Alzueta. Influence of pressure on H_2S oxidation. Experiments and kinetic modeling. Fuel 2019;258:116145.

[41] MU Alzueta, R Pernía, M Abián, Á Millera, R Bilbao. CH_3SH conversion in a tubular flow reactor. Experiments and kinetic modelling. Flame 2019;203:23–30.

[42] MU Alzueta, R Bilbao, P Glarborg. Inhibition and sensitization of fuel oxidation by SO_2. Combust Flame 2001;127:2234–2251.

[43] M Abián, M Cebrián, Á Millera, R Bilbao, MU Alzueta. CS_2 and COS conversion under different combustion conditions. Combust Flame 2015;162:2119–2127.

[44] M Abián, Á Millera, R Bilbao, MU Alzueta. Impact of SO_2 on the formation of soot from ethylene pyrolysis. Fuel 2015;159:550–558.

[45] CL Rasmussen, JG Jakobsen, P Glarborg. Experimental measurements and kinetic modeling of CH_4/O_2 and $CH_4/C_2H_6/O_2$ conversion at high pressure. Int J Chem Kinet 2008;40:778–807.

[46] X Zheng, EM Fisher, FC Gouldin, JW Bozzelli. Pyrolysis and oxidation of ethyl methyl sulfide in a flow reactor. Combust Flame 2011;158:1049–1058.

[47] R Van de Vijver, NM Vandewiele, AG Vandeputte, KM Van Geem, M-F Reyniers, WH Green, et al. Rule-based ab initio kinetic model for alkyl sulfide pyrolysis. Chem Eng J 2015;278:385–393.

[48] CHEMKIN-PRO 15151, Reaction Design, San Diego, (2013).

[49] J Giménez-López, Á Millera, R Bilbao, MU Alzueta. Experimental and kinetic modeling study of the oxy-fuel oxidation of natural gas, CH_4 and C_2H_6. Fuel 2015;160:404–412.

[50] Z Zeng, BZ Dlugogorski, I Oluwoye, M Altarawneh. Co-oxidation of methane (CH_4) and carbon disulfide (CS_2). Proc Combust Inst 2019;27:677–685.

[51] Z Zeng, M Altarawneh, I Oluwoye, P Glarborg, BZ Dlugogorski. Inhibition and Promotion of Pyrolysis by Hydrogen Sulfide (H_2S) and Sulfanyl Radical (SH). J Phys Chem A 2016;120:8941–8948.

[52] R Zhu, C-C Hsu, MC Lin. Ab initio study of the $CH_3 + O_2$ reaction: kinetics, mechanism and product branching probabilities. J Chem Phys 2001;115:195–203.

[53] CL Rasmussen, AE Rasmussen, P Glarborg. Sensitizing effects of NO_x on CH_4 oxidation at high pressure. Combust Flame 2008;154:529–545.

[54] NK Srinivasan, MC Su, JW Sutherland, JV Michael. Reflected shock tube studies of high-temperature rate constants for $CH_3 + O_2$, $H_2CO + O_2$, and $OH + O_2$. J Phys Chem A 2005;109:7902–7914.

[55] C-L Yu, C Wang, M Frenklach. Chemical kinetics of methyl oxidation by molecular oxygen. J Phys Chem 1995;99:14377–14387.

[56] SM Hwang, S-O Ryu, KJ De Witt, MJ Rabinowitz. Rate coefficient measurements of the reaction $CH_3 + O_2 = CH_3O + O$. J Phys Chem A 1999;103:5949–5958.

[57] JT Herbon, RK Hanson, CT Bowman, DM Golden. The reaction of $CH_3 + O_2$: experimental determination of the rate coefficients for the product channels at high temperatures. Proc Combust Inst 2005;30:955–963.

[58] RX Fernandes, K Luther, J Troe. Falloff curves for the reaction $CH_3 + O_2(+M) = CH_3O_2(+M)$ in the pressure range 2–1000 bar and the temperature range 300–700 K. J Phys Chem A 2006;110:4442–4449.

[59] NK Srinivasan, MC Su, JV Michael. $CH_3 + O_2 = H_2CO + OH$ Revisited. J Phys Chem A 2007;11:11589–11591.

[60] Y Song, L Marrodán, N Vin, O Herbinet, E Assaf, C Fittschen, et al. The sensitizing effects of NO_2 and NO on methane low temperature oxidation in a jet stirred reactor. Proc Combust Inst 2019;37:667–675.

[61] WK Metcalfe, SM Burke, SS Ahmed, HJ Curran. A hierarchical and comparative kinetic modeling study of C1–C2 hydrocarbon and oxygenated fuels. Int J Chem Kinet 2013;45:638–675.

[62] DL Baulch, CT Bowman, CJ Cobos, RA Cox, T Just, JA Kerr, et al. Phys Chem Ref Data 2005;34:1244.